Electronic Supplementary Material (ESI) for Materials Advances.

Supporting Information

Top-Down Surfactant-Free Electrosynthesis of Magnéli phase Ti_9O_{17} Nanowires

Peter M. Schneider[1,⊥], Christian M. Schott[1,⊥], Dominik Maier[1], Sebastian A. Watzele[1], Jan Michalička[2], Jhonatan Rodriguez-Pereira[2,3], Ludek Hromadko[3], Jan Macak[2,3*], Volodymyr Baran[4], Anatoliy Senyshyn[5], Arnaud Viola[6], Frédéric Maillard[6], Elena L. Gubanova[1*] and Aliaksandr S. Bandarenka[1,7*]

1 - Physics of Energy Conversion and Storage, Technical University of Munich, James-Franck-Str. 1, 85748 Garching, Germany

2 - Central European Institute of Technology, Brno University of Technology, Purkynova 123, 61200 Brno, Czech Republic,

3 - Center of Materials and Nanotechnologies, University of Pardubice, Nam. Cs. Legii 565, 53002 Pardubice, Czech Republic,

4 - Deutsches Elektronen Synchrotron (DESY), Notkestr. 85, 22607 Hamburg, Germany

5 - Heinz Maier-Leibnitz Zentrum (MLZ), Technische Universität München, Lichtenbergstr. 1, 85748, Garching, Germany,

6 - Univ. Grenoble Alpes, Univ. Savoie Mont Blanc, CNRS, Grenoble INP[⊥], LEPMI, 38000 Grenoble, France, [⊥]Institute of Engineering and Management Univ. Grenoble Alpes,

7 - Catalysis Research Center TUM, Ernst-Otto-Fischer-Str. 1, 85748 Garching, Germany

* Corresponding Authors: E-mails: Jan.Macak@ceitec.vutbr.cz (J. Macak), elena.gubanova@tum.de (E. Gubanova) bandarenka@ph.tum.de (A.S. Bandarenka)

⊥ P.M. Schneider and C.M. Schott contributed equally to this work.

Synthesis. To synthesize TiO_x nanostructures, a method, called electrochemical erosion, was applied. The choice of appropriate synthesis parameters is essential since it strongly affects the erosion of bulk wires. This allows tuning the nanostructures obtained *via* adjustment of methodological parameters, such as electrolyte composition, concentration, applied potential signal type, amplitude, and frequency (in the case of alternating current (AC)). For the TiO_x nanostructures produced in our study, we applied a voltage signal to bulk Ti wires (Ø 0.25 mm, 99.6 %, MaTecK, Germany) using a VSP 300 potentiostat (Bio-Logic, France). For each synthesis, two fresh Ti wires were used. The influence of the AC frequency and electrolyte composition on the morphology, size, and properties of the TiO_x nanostructures was investigated to obtain the ideal electrochemical erosion parameters for the synthesis of ultrafine TiO_2 nanowires with high surface area. We applied a sinusoidal AC signal for each synthesis with a potential amplitude fixed to 25 V. The Ti wires were immersed in the electrolyte solution until a current of up to 2 A was reached, which is equal to an immersion depth of each wire of approximately 5 mm. In the following, we

present the significant effect of changing the electrolyte cation from K^+ to Na^+ and the anion from OH^- to Cl^- on the erosion of titanium. 1 M KCl (ACS reagent, 99.0-100.5 %, Sigma-Aldrich, Germany), saturated NaOH (99 %, Grüssing, Germany), and saturated KOH (85 %, Grüssing, Germany) served as electrolytes. Exemplary, for the synthesis of Ti_9O_{17} nanowires,50 mL of freshly prepared saturated KOH electrolyte was poured into a flat Teflon cell, specifically designed for the erosion of bulk Ti wires in alkaline media. The two wires were immersed into the solution with a depth of ~ 5 mm, as mentioned above, and a wire-to-wire separation distance of ~ 20 mm. During the erosion, the immersion depth of the bulk Ti wires was kept constant to ensure continuous production of Ti_9O_{17} nanowires. The synthesis was stopped after the desired mass of eroded Ti was reached, obtained from weighing the mass of bulk Ti wires before and after synthesis. Afterward, the obtained suspension was filtered in a Büchner funnel, washed with a mixture of ultrapure water (18.2 MΩcm, Merck Millipore, USA) and ethanol (EMSURE® ACS, ISO, Reag. Ph Eur, Sigma Aldrich®, USA), and dried in a furnace for 12 h at 60°C in air.

Influence of electrolyte and AC frequency. From SEM analysis in **Figure S1**, it is evident that the TiO_x nanostructure morphology varies strongly among the 3 different electrolytes. **Figure S1a** shows the TiO_x nanostructure generated in 1 M KCl, which exhibits a porous structure with non-uniform aggregates. No formation of nanowires or nanoparticles could be observed. **Figure S1b** shows SEM images of the sample eroded in saturated NaOH. In this case, the size of the TiO_x nanostructures increases significantly and exhibits a “cloudy” structure. Only changing the cation of the electrolyte from Na^+ to K^+, while keeping the OH^- as the anion, yields nanowires as a synthesis product with a defined nanostructure, as depicted in **Figure S1c**. Changing the frequency of the AC signal from 200 Hz to 100 Hz and 20 Hz using the same saturated KOH electrolyte does

not yield significant differences. In each case, nanowires were fabricated, which show similar lengths and diameters.

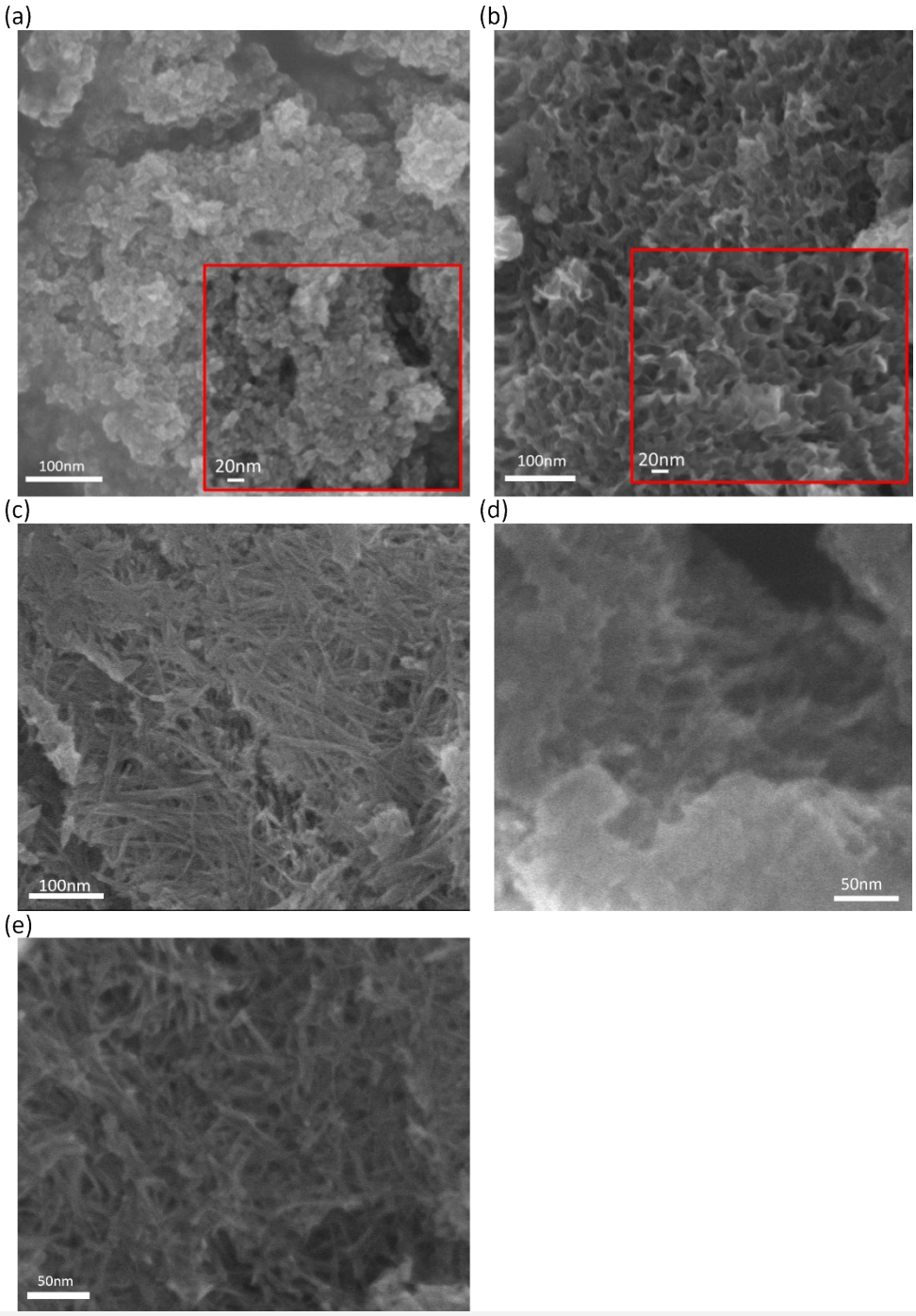

Figure S1. *(a) and (b) Exemplary SEM images of TiO_x nanostructures synthesized in 1 M*

KCl and saturated NaOH, respectively. Both samples were synthesized using a sinusoidal voltage signal with a 25 V amplitude and an AC frequency of 200 Hz. (c), (d), and (e) SEM images of TiO_x nanowires synthesized in saturated KOH with 200 Hz, 100 Hz, and 20 Hz AC frequency, respectively.

Figures S2a and **S2b** illustrate the nitrogen adsorption/desorption isotherms of the TiO_x nanostructures synthesized in saturated KOH, 1 M KCl, and saturated NaOH. Due to the successful synthesis of Ti_9O_{17} nanowires for saturated KOH, the AC frequency was changed from 200 Hz to 100 and 20 Hz to study this synthesis parameters' effect on the nanowires. **Figure S2c** shows a bar chart with the evaluated BET surface areas corresponding to approximately 133 m^2/g and 16 m^2/g for TiO_x nanostructures synthesized in 1 M KCl and saturated NaOH, respectively. Changing the AC frequency in saturated KOH solution yields nanowires with similar BET surface area, i.e., ~ 215 m^2/g, ~ 170 m^2/g, and ~ 208 m^2/g for 200 Hz, 100 Hz, and 20 Hz, respectively. These findings coincide with the findings obtained from the SEM characterization, presented in **Figure S1**. The nanostructures synthesized in saturated NaOH increased drastically in size, resulting in a significantly smaller surface compared to the support materials synthesized in 1 M KCl and saturated KOH. The increase in BET surface area of Ti_9O_{17} synthesized in saturated KOH by a factor of ~ 1.7 compared to the sample in 1 M KCl can be explained by the presence of the ultrathin nanowire network in the KOH sample. The similar BET surface areas of the nanowires synthesized by different AC frequencies in saturated KOH confirmed the SEM investigation depicted in **Figure S1c** to **S1e** showing very similar sizes and structures of the nanowires.

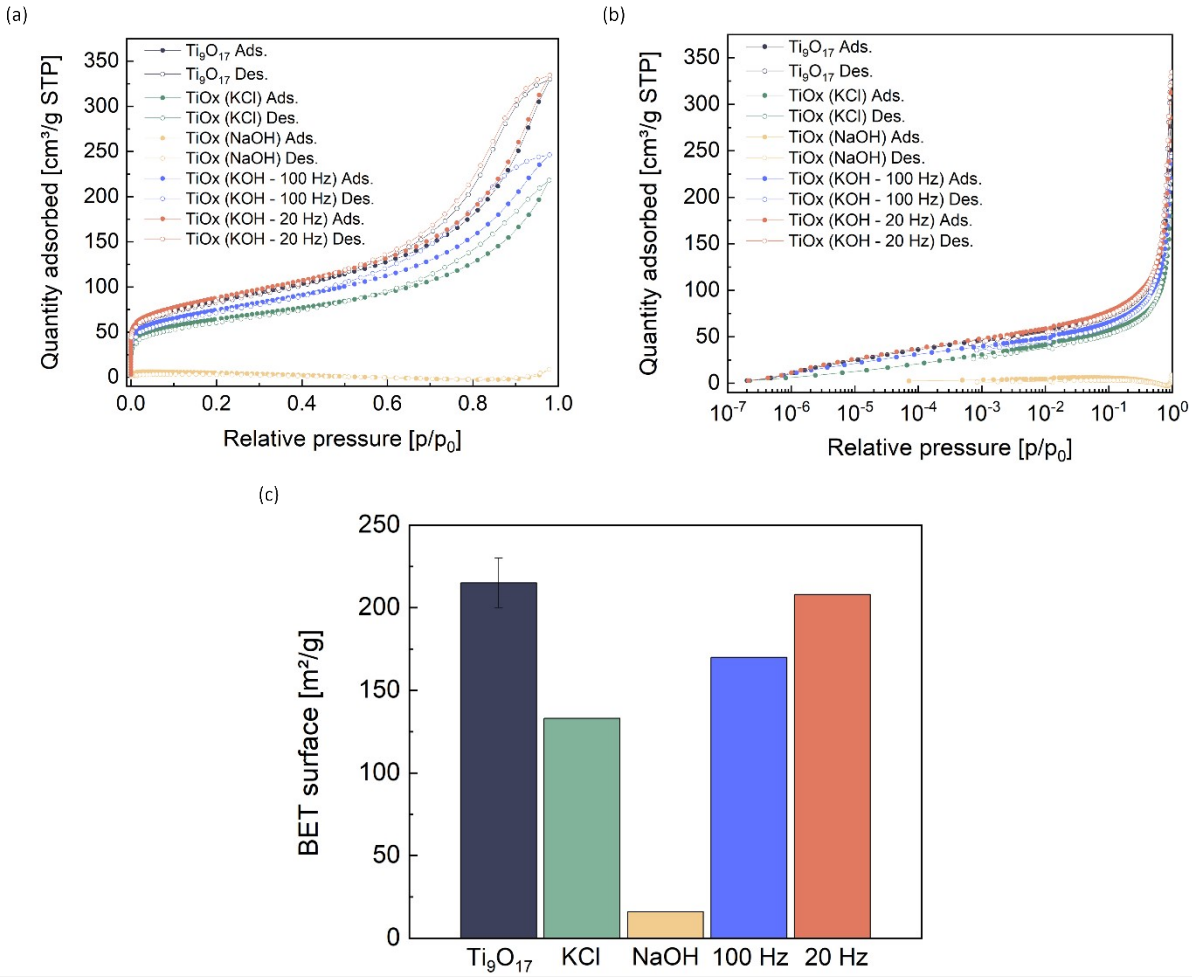

Figure S2. *(a) N_2 adsorption and desorption isotherms of TiO_x nanostructures synthesized in different electrolytes (KOH/KCl/NaOH) and with different AC frequencies (100 Hz/20 Hz in KOH). (b) Semi-log plot of isotherms depicted in (a). (c) BET surface area plot for comparison of synthesized samples.*

Figure S3a-b and **S3c-d** display the 2p1/2 and 2p3/2 doublet peaks for titanium and oxygen for the TiO_x nanostructures synthesized in 1 M KCl and saturated NaOH, respectively. From region quantification, the atomic concentration ratio of potassium or sodium, oxygen, and titanium can be calculated, corresponding to 1:50:18 and 1:3:1 for the nanostructures synthesized in 1 M KCl and saturated NaOH, respectively. The ratio indicates a minimal residue of potassium in the case

of KCl. However, in the case of NaOH, we detect significant quantities of sodium within the synthesized nanostructures. Additionally, the components' quantification allows us to determine the ratio of Ti in different oxidation states, focusing mainly on 3^+, 4^+, and neglectable amounts of non-stoichiometric $Ti^{\delta+}$. The Ti^{3+}:Ti^{4+} ratio corresponds to 1:20 and 1:17 for the nanostructures synthesized in 1 M KCl and saturated NaOH, respectively indicating TiO_2-like nanostructures for KCl and NaOH.

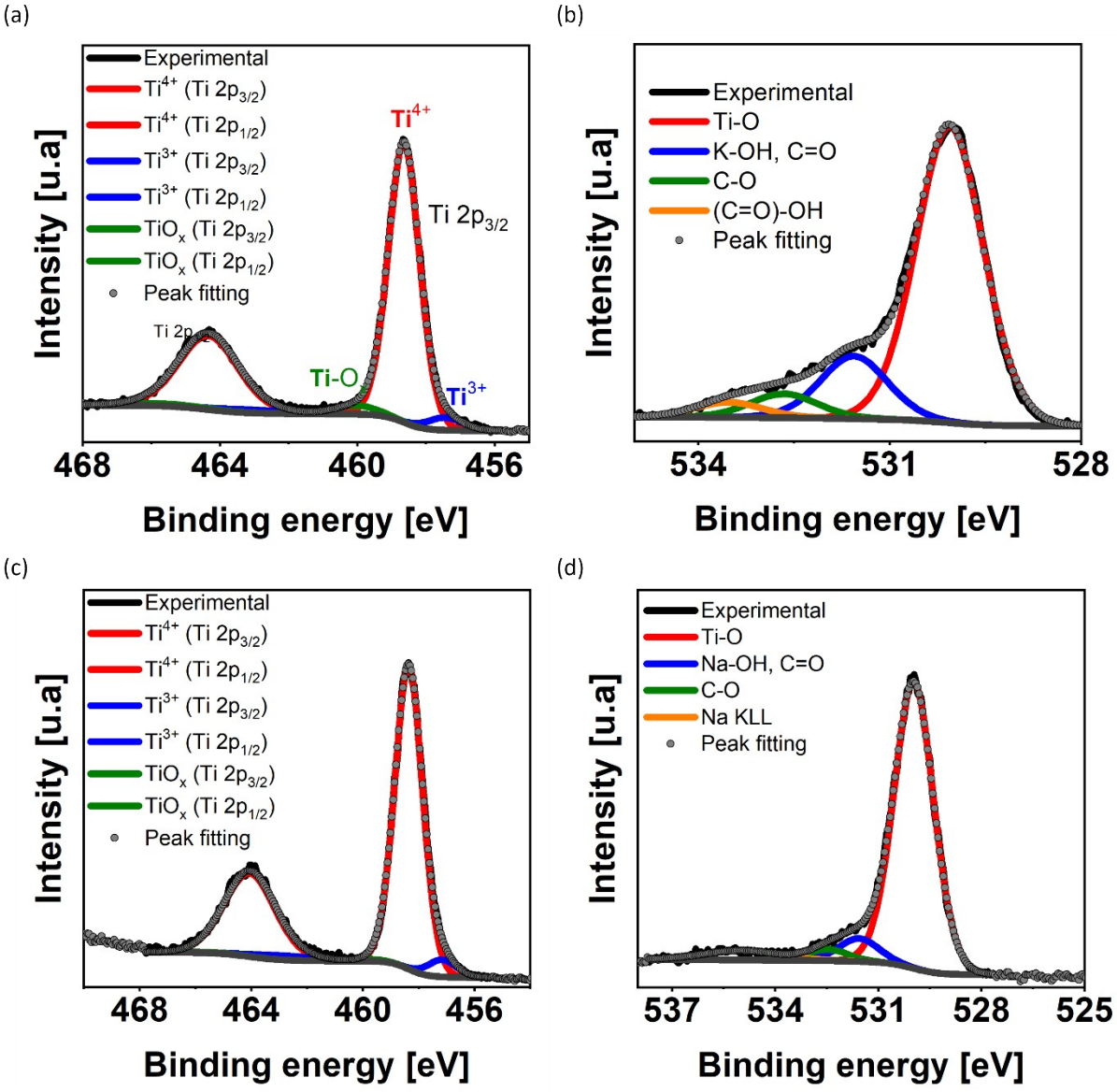

Figure S3. *XPS spectra of the TiO_x nanostructures synthesized in (a-b) 1 M KCl and (c-d) saturated NaOH displaying the $2p_{1/2}$ and $2p_{3/2}$ doublet peaks for titanium (Ti 2p) and oxygen (O 1s), respectively. Fitting of the peaks indicates the presence of Ti with different oxidation states and different oxygen compounds.*

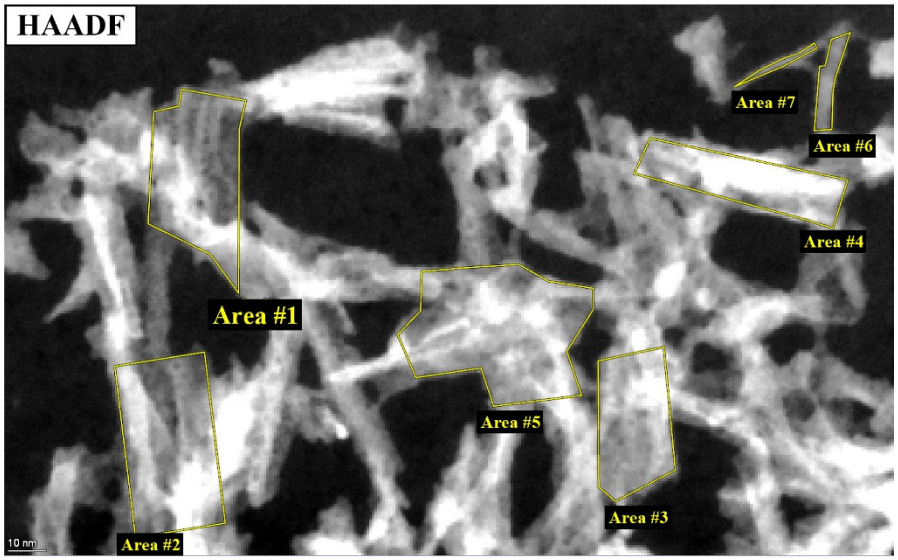

Figure S4. *STEM-HAADF image where EDX analysis was performed (Figure 2c-f).*

Area	Element	Atomic Fraction (%)	Atomic Error (%)
#1	O	66.17	3.38
	K	3.84	0.68
	Ti	29.98	3.55
#2	O	66.47	3.32
	K	4.32	0.76
	Ti	29.22	3.5
#3	O	66.02	3.3
	K	4.87	0.85
	Ti	29.11	3.5
#4	O	67.52	3.3
	K	3.9	0.69
	Ti	28.57	3.46
#5	O	66.12	3.31
	K	4.64	0.81

	Ti	29.24	3.5
#6	O	69.66	3.16
	K	3.89	0.69
	Ti	26.45	3.3
#7	O	69.16	3.26
	K	3.4	0.65
	Ti	27.44	3.39

Table S1. *Chemical composition measured from selected areas containing TiO_2-like nanowires marked in* ***Figure S4****.*

All investigated samples are weakly scattering, where collected diffraction signal from XRD and PDF mode is dominated by air scattering. For sake of clarity, the diffraction signal of empty capillary/air was subtracted for all plotted XRD patterns. The character of the diffraction signal was rather different for the samples synthesized in KCl and NaOH. Nanostructured TiO_x synthesized in 1 M KCl can be described by the contribution of three TiO_2 polymorphs, namely rutile, anatase, and brookite, as shown in **Figure S5a**. The weight percentages of the three phases correspond to 10%, 45%, and 45% w/w, respectively. The average crystallite sizes for rutile, anatase, and brookite in the sample were determined as 92, 67, and 84 Å, accordingly, by modeling the diffraction peak width with Gaussian size distribution. The diffraction pattern for TiO_x synthesized in saturated NaOH shows similar results to that of the nanowires synthesized in saturated KOH, namely non-stoichiometric TiO_x in the form of Ti_9O_{17} and metallic (hcp) titanium (see **Figure S5b**). The average crystallite size was determined as large as 77 Å, which is close to the value for the nanowires synthesized in saturated KOH (74 Å). Examining the G(r) functions obtained from PDF data, we could clearly distinguish between TiO_x synthesized in 1 M KCl and saturated NaOH (see **Figure S5c**), which is reflected in the shift of the characteristic correlation

maxima (e.g., at 3.0 Å, 3.6 Å, 4.6 Å, etc.) towards higher r. By comparison of the position of the first correlation maxima at low r values to the tickmarks in the inset figure of **Figure S5c**, we can exclude the presence of TiO, i.e., the presence of significant amounts of Ti^{2+} in our samples. Moreover, the results from PDF indicate a crystal structure close to anatase TiO_2 for both TiO_x synthesized in saturated NaOH and 1 M KCl.

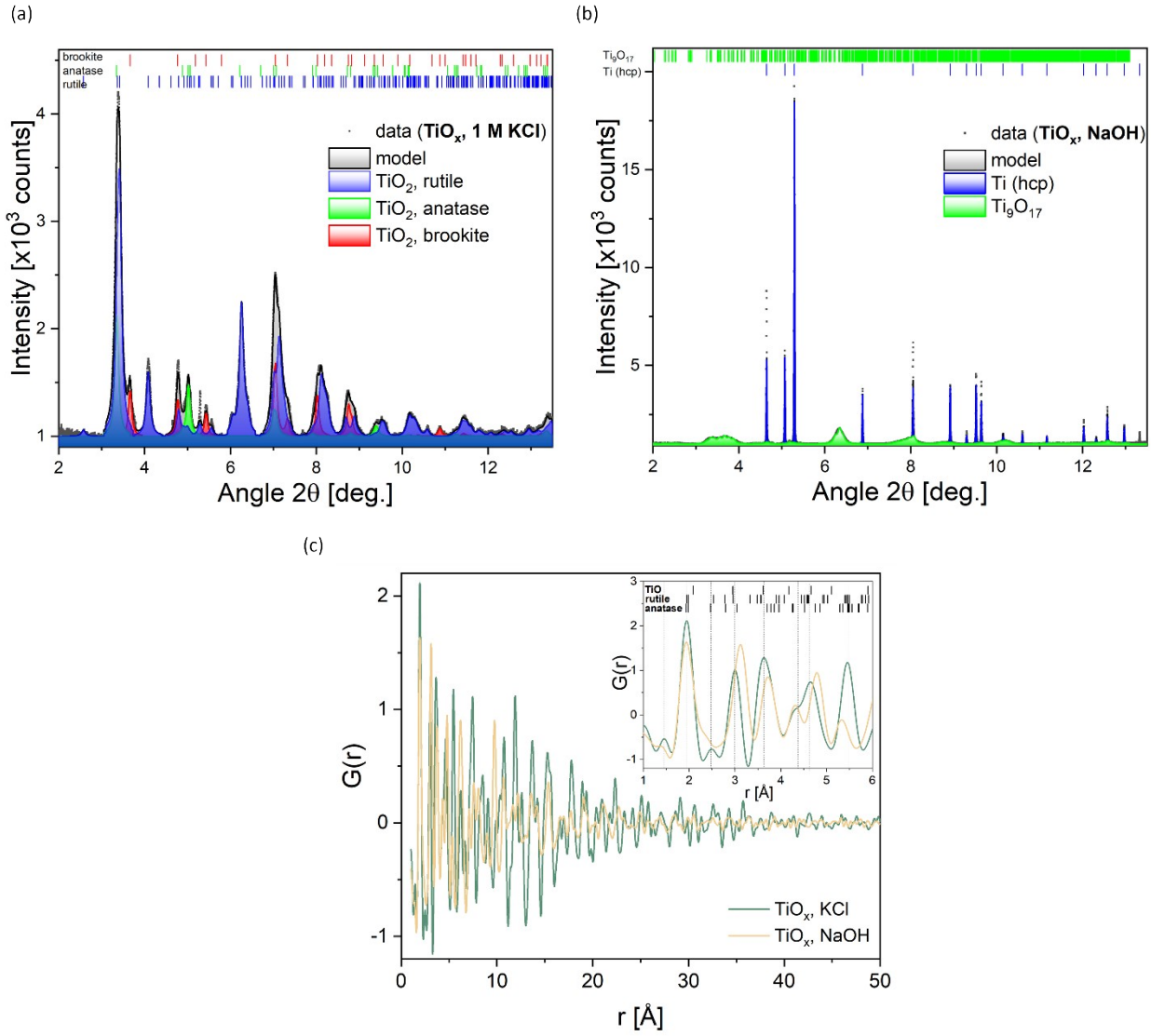

Figure S5. *(a) and (b) background subtracted XRD patterns and graphical results of their modeling for TiO_x nanostructures synthesized in KCl and NaOH, respectively. Contributions from*

different phases are displayed by color; vertical tickmarks correspond to the calculated Bragg reflection positions. (c) Pair distribution function G(r) determined from diffraction data in PDF mode. Dashed vertical lines correspond to the maximum peaks for the TiO_x sample synthesized in KCl; small tickmarks illustrate interatomic distances in parent TiO_2 rutile, anatase, and TiO.

In contrast to TiO_x nanostructures synthesized in KCl, which could be modeled using a combination of anatase, rutile, and brookite, the ones prepared using NaOH revealed no clearly distinguishable anatase, rutile, and brookite signals, but a reflection splitting different to that observed for TiO_x nanostructures synthesized in KCl.

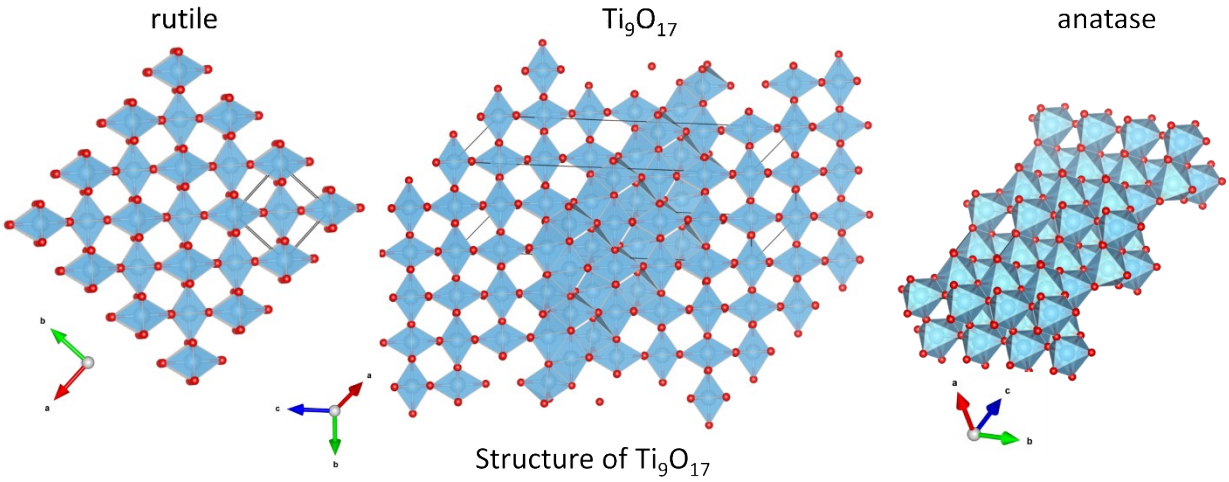

Figure S6. *Crystal structure of rutile (left) and anatase (right) TiO_2 and non-stoichiometric TiO_2, i.e., Ti_9O_{17} (middle). The crystal structure of Ti_9O_{17} exhibits the typical characteristic of Magnéli phases TiO_2 - a layered rutile structure separated by shear layers.*